INTRUSIVE EXPERIENCES IN POST-TRAUMATIC STRESS DISORDER: TREATMENT RESPONSE INDUCES CHANGES IN THE EFFECTIVE CONNECTIVITY OF THE ANTERIOR INSULA

Abbreviated title:

Insular Cortex Influence on Intrusivity

Author list:
Arnaud **Leroy**[1,2,3*], Etienne **Very**[4,5], Philippe **Birmes**[5], Sébastien **Szaffarczyk**[1], Renaud **Lopes**[6,7], Cécile **Faure**[1], Stéphane **Duhem**[2,3], Pierre **Grandgenèvre**[2], Frédérique **Warembourg**[2], Guillaume **Vaiva**[1,2,3], Renaud **Jardri**[1,8]

Affiliations :

1. Univ Lille, INSERM, CHU Lille, Lille Neuroscience & Cognition Centre (U-1772), Plasticity & SubjectivitY team, CURE platform, 59000 Lille, France
2. CHU Lille, Fontan Hospital, General Psychiatry Dpt., 59037 Lille cedex, France
3. Centre National de Ressources et Résilience pour les psychotraumatismes (CN2R Lille - Paris), 59000 Lille, France
4. CHU Toulouse, Purpan Hospital, Psychiatry Department, 31059 Toulouse Cedex, France
5. ToNIC, Toulouse NeuroImaging Center, INSERM U-1214, UPS, France
6. Univ Lille, INSERM, CHU Lille, Lille Neuroscience & Cognition Centre (U-1772), Degenerative & Vascular Cognitive Disorders team, 59000 Lille, France
7. Univ Lille, CNRS, INSERM, CHU Lille, Institut Pasteur de Lille, US 41 - UMS 2014 - PLBS, 59000 Lille, France
8. CHU Lille, Fontan Hospital, Child & Adolescent Psychiatry Dpt., 59037 Lille cedex, France

Corresponding Author: *, arnaud.leroy@chru-lille.fr

Number of display items: 3 figures/ 2 tables + 6 suppl. items

Number of words: 3570

Statement of interest: AL is consultant for Kinnov Therapeutics. RJ has been invited to scientific meetings, and boards with compensation, by Lundbeck, Janssen and Otsuka. None of these links of interest are related to the present work.

ABSTRACT (251 words)

Introduction: One of the core features of posttraumatic stress disorder (PTSD) is reexperiencing the trauma. Th anterior insula (AI) was proposed to play a crucial role in these intrusive experiences. However, the dynamic function of the AI in reexperiencing trauma, as well as its putative modulation by effective therapy, still need to be specified.

Methods: Thirty PTSD patients were enrolled and exposed to chemo-facilitated traumatic memory reactivation therapy. Resting-state fMRI scans were acquired before and after treatment. To explore AI directed influences over the rest of the brain, we referred to a mixed-model using pre/post Granger causality analysis seeded on the AI as a within-subject factor and treatment response as a between-subject factor. To further identify correlates of reexperiencing trauma, we investigated how intrusive severity affected : (i) causality maps and (ii) the spatial stability of other intrinsic brain networks.

Results: We observed dynamic changes in AI effective connectivity in PTSD patients. Many within- and between-network causal paths were found to be less influenced by the AI after effective therapy. Insular influences were found positively correlated with flashback severity, while reexperiencing was linked with a stronger *default mode network* (DMN) and more unstable *central executive network* (CEN) connectivity.

Discussion: We showed that directed changes in AI signalling to the DMN and CEN at rest may underlie the degree of intrusive symptoms in PTSD. A positive response to treatment further induced changes in network-to-network anticorrelated patterns. Such findings may guide targeted neuromodulation strategies in PTSD patients not suitably improved by conventional treatment.

Key-words:

Post-Traumatic Stress Disorder; Propranolol; Therapeutics; salience network; fMRI

INTRODUCTION

Posttraumatic stress disorder (PTSD) is a disabling condition that can be triggered by terrifying events that have the potential to disrupt life, such as interpersonal violence, combat, life-threatening accidents or disasters, as well as global pandemics (1). PTSD may lead to chronic psychiatric or addictive morbidities, loss of normal daily functioning, and increased risk of suicide (2). This disorder usually induces intrusive symptoms (i.e., distressing recollections of the event, including flashbacks and nightmares, often called "reexperiences"), persistent avoidance of stimuli associated with the trauma, negative alterations in cognitions or mood, and hyperarousal (3). "Reexperiencing" is considered central in the pathophysiology of PTSD, despite some similarities with other intrusive thoughts observed transdiagnostically, such as hallucinations, ruminations or persistent worries (4–7). Even if this research field is prolific, it still lacks a common neurofunctional signature for intrusive experiences that adequately circumscribes the underlying mechanisms of PTSD.

Brain-wide dysconnectivity has been suggested at the root of several psychiatric disorders, and key structures have picked the interest of PTSD scientists. Among the candidate nodes, the anterior insula (AI) was identified as one of the major connector hubs in the brain (8). This structure has been implicated in a large variety of functions, ranging from feelings representation to bodily and self-awareness (9). The AI receives convergent inputs from multiple sensory modalities, including the auditory and visual systems (10–14), and converging evidence supports its involvement in simultaneous attention to multisensory events (15,16). The AI was also proposed to tag salient endogenous and external information and further reallocate attentional resources towards them (17), making it a central element of the "salience network" (SN).

On a more pathological side, hyperarousal and re-experiencing were shown to be associated with increased activity in the bilateral AI and connected limbic structures, such as the amygdala (18) or the hippocampus (19). These symptoms were also associated with an increased functional connectivity of the SN network as a whole (20). Interestingly, aberrant SN effective connectivity was

also proven involved in the process of switching from a state of unconstrained rest to one of experiencing hallucinatory events in schizophrenia patients (21), reinforcing the idea that this network may govern intrusive experiences in general.

In this vein, the SN is thought to tightly control the balance between various intrinsic networks and to swiftly move from rest to task-based actions and vice-versa, a theory that has been conceptualized as the tripartite model (17,22). According to this framework, the SN may drive commonly observed anticorrelated patterns between the default mode network (DMN, underlying self-referential processes) and the central executive network (CEN, involved in cognitive control and decision making), an interaction already shown to be impaired in PTSD. For instance, aberrant increases in SN and decreased DMN functional connectivity were described in PTSD patients (20), whereas a surge in connectivity strength of the CEN was reported to be associated with intrusiveness (23). Though these findings are encouraging, some gaps remain, such as the exact links between AI dysconnectivity and other biological theories of PTSD.

At the microscale level, we indeed know that SN activation is mediated by the B-noradrenergic system. In particular, activation of the locus coeruleus, the main source of epinephrine secretion in the brain, was found to be involved in SN activation (24). The administration of drugs increasing the epinephrine level has also been linked with SN activation (25,26), whereas the administration of propranolol, a noradrenergic beta-receptor blocker, deactivates the SN (27). Finally, a genetic study revealed that only carriers of a common functional deletion in ADRA2B, a gene coding for the α2b-adrenoreceptor, displayed increased phasic amygdala responses under stress (28), again supporting the existence of an association between salience responses and B-noradrenergic regulation.

Interestingly, trauma memory reactivation therapy performed under the influence of propranolol (considered a putative reconsolidation blocker) was recently found to reduce symptom severity in PTSD (29). Referring to a similar randomized controlled trial (RCT) design, the present study intends to bring new insight to the dynamic role of the SN in PTSD and, more specifically, to circumscribe the

directed influence of AI over the rest of the brain as a function of treatment response. We hypothesize that such chemo-facilitated treatment can modulate the effective connectivity of AI and that these plastic changes correlate with a reduction in trauma reexperiencing symptoms. In reference to the tripartite model, we also expect this downgrading in intrusiveness to be linked to changes in DMN and CEN spatial stability, demonstrating a brain-wide reallocation of cognitive resources in PTSD patients who respond to treatment.

MATERIALS AND METHODS

Population

Thirty patients with a primary diagnosis of PTSD according to DSM-IV-TR criteria (Structured Clinical Interview for DSM-IV, PTSD module) provided written informed consent to participate in the research (**Table 1**). They were all taken from a RCT testing for the efficacy of traumatic memory reactivation under the influence of propranolol versus placebo one week posttreatment. This trial received approval from an ethics committee (CPP 2009-012976-29) and was registered on clinicaltrials.gov (NCT01713556). The main results for this clinical trial are presented elsewhere (30).

Participants waiting for treatment were randomly and blindly allocated to two experimental groups (1:1 ratio): (i) a "propranolol" group, receiving traumatic memory reactivation + propranolol, and (ii) a "placebo" group, receiving traumatic memory reactivation + placebo. Propranolol or placebo was administered 90-minutes before a brief memory reactivation session, performed once a week for 6 consecutive weeks. The *Posttraumatic Stress Disorder Checklist Scale* - PCL-S (31) was used to quantify symptom severity and assess treatment response. Because we were interested in intrusive symptoms, we focused on the item sum of PCL-S Q1-to-Q5 (31). Assessment was made before treatment (V1) and one week after the end of the treatment (V7). The response to treatment

was considered positive for at least a 30% decrease (32,33) in the PCL-S Q1-to-Q5 score compared to baseline.

MRI acquisition and data preprocessing

Patients underwent two MRI sessions at rest with their eyes closed (at V1 and V7) on a 3T Philips Achieva scanner with an 8-channel head coil. Each of these sessions included a 4-min T1-weighted (T1w) 3D anatomical run (124 transverse slices, field of view = 256 mm^3, vox = 0.8 mm^3) and a 15-min T2*-weighted 3D-PRESTO sequence (34–36). This functional sequence (dynamic scan time = 1000 ms, TE = 9.6 ms, flip angle = 9°, vox = 3.3 mm^3) allowed for full functional brain coverage with a temporal resolution particularly suited for effective connectivity analysis (37).

Anatomical and functional MRI data were preprocessed using the FMRIPrep pipeline v. 1.5 (38), a Nipype v. 1.2.2 based tool (39). T1w images were corrected for nonuniform intensity and skull stripped. Brain tissue segmentation of cerebrospinal fluid, white-matter and gray-matter was performed on the brain-extracted T1w image. Volume-based spatial normalization to the *Montreal Neurological Institute* ICBM-152 (MNI) template was performed through nonlinear registration using brain-extracted versions of both the T1w reference and the MNI template.

For functional images, a reference BOLD volume and its skull-stripped version were generated and coregistered to the T1w image using a boundary-based registration algorithm with 9 degrees of freedom. Head-motion parameters were estimated before spatiotemporal filtering. Motion correction, BOLD-to-T1w transformation and T1w-to-template (MNI) warps were concatenated and applied in a single step using antsApplyTransforms (ANTs v2.1.0) based on Lanczos interpolation. Spatial smoothing with a 6-mm isotropic Gaussian kernel was then performed, and a second "nonaggressive" denoising step was conducted using independent component analysis [ICA-AROMA]. Linear trends were finally removed, and a high-pass temporal filtering with 3 cycles/point was applied.

Granger causality analysis

Effective connectivity was assessed using Granger causality analysis (GCA), which allows for the data-driven exploration of a reference region's influence over the brain as well as targets of influence on the same given area (40). We used this approach to account for the multiple regions naturally connected to the SN (41) and to avoid missing brain areas that could not have been retained in a more traditional theory-driven framework. Here, we used the implementation proposed in the BrainVoyager software suite (v21.4, BrainInnovation, Maastricht; *Granger Causality Mapping* plugin v1.5). We defined the bilateral AI, according to the meta-analysis from Laird et al. (**Figure 1**) (2011) (42) , as the reference region for later analyses. GCA maps were used to visualize the directed influences between the AI and every voxel in both directions after applying a gray-matter mask. These maps were thresholded using a false-discovery rate approach at q-levels of 0.01. We finally tested the association between GCA maps and symptom severity at the V7 time-point, considering $p_{fwe}<0.05$ as significant.

Main statistical analysis

To assess changes in AI effective-connectivity pre/post treatment between patients who respond to treatment (responders) and those who did not (nonresponders), we referred to a 2x2 mixed-model ANOVA, using GCA maps at V1 and V7 as within-subject factors and treatment response as a between-subject factor. Post-hoc analyses used Student's t-tests. All maps were then thresholded using a cluster-based permutation method (43). To prevent potential inflated false-positive rates (44), we first specified a cluster-defining threshold (CDT) at $p_{uncorrected} < 0.001$. After conducting a 1000-iteration Monte-Carlo simulation, a cluster-extent threshold was defined as a value high enough to keep the family-wise error at $p_{fwe}=0.05$. The resulting brain areas were labeled using the Anatomy toolbox v 3.0 (https://github.com/inm7/jubrain-anatomy-toolbox, (45)).

Intrinsic network spatial stability measure

In parallel, we also explored the spatial stability of the DMN and the CEN posttreatment (i.e., the V7 time-point) using a "goodness-of-fit" (GoF) procedure. After decomposing each posttreatment functional dataset using *independent component analysis* (ICA), we selected the components exhibiting the highest spatial correlation with an a priori template. For each participant, this procedure was repeated twice : with the DMN and the CEN template, respectively (46). The resulting GoF scores were assumed to reflect posttreatment DMN and CEN spatial stability. We tested for an association between these scores and the severity of intrusive symptoms using Pearson's *r* correlation test, considering $p<0.05$ as significant.

RESULTS

Demographic and clinical variables

At baseline, responders and nonresponders were comparable in terms of (i) sociodemographic characteristics (age and sex-ratio), and (ii) symptom severity (PCL-S scores/subscores and depressive symptoms measured with the *Beck Depression Inventory* (47)). Note that, counterintuitively, the responder group contained fewer patients receiving propranolol (see (30) for a more detailed description of the RCT main findings).

Table 1: Population description

	Responders (n=16)	**Nonresponders (n = 14)**
Age	41.3 (12.3)	36.6 (13.5)
Sex (Male /Female)	7/9	8/6
Dvars	24.3 (3.74)	24.1 (4.05)
Global signal	887 (121)	916 (96.3)
Total PCL-S score	65.4 (9.34)	68.4 (9.34)
PCLS-score (question 1 to 5)	18.9 (3.38)	19.4 (3.38)
Beck Depression inventory score	25.9 (14.5)	28.9 (11.3)
*Rate of patients receiving propranolol **	*31.3 %*	*78.6%*

*p <0.05.

INSERT FIGURE 1 ABOUT HERE

AI effective connectivity at V1

GCA performed on the whole-sample at baseline revealed that the bilateral AI significantly modulates a group of regions involved in motor preparation, execution and action monitoring (i.e., precentral gyrus, the supplementary motor area, the left thalamus, and the frontal pole), as well as in visuospatial processing (i.e., the paracingulate gyrus and the precuneus). See **Figure 1** and **Suppl. Table 1**. No specific connectivity differences were evidenced between the responder and nonresponder groups before treatment.

AI effective-connectivity changes between V1 and V7

The mixed-model ANOVA revealed significant changes in AI causal maps after treatment. A significant [time-point x group] interaction was evidenced: (i) laterally, in the mid- and posterior insula, amygdala, precentral gyrus and supramarginal gyrus ; and (ii) medially, in the cingulate cortex (anterior and posterior) and the precuneus (**Suppl. Table 2**). Compared with nonresponders, patients showing clinical improvement exhibited a reduced influence of the AI over a wide socioemotional network composed of the superior frontal gyrus, anterior and posterior supramarginal gyri, anterior and posterior cingulate, central operculum and right amygdala. Conversely, responders exhibited a higher influence of the AI over the precuneus (Cf. **Figure 2**, **Table 2**). Simple pre/posttreatment contrasts for responders and nonresponders are available in **Suppl. Figures 1, 2** and **Suppl. Tables 3, 4** respectively, whereas significant results for propranolol vs placebo at V7 are presented in **Suppl. Table 5**.

Regression analysis conducted posttreatment further revealed that the more severe the intrusive symptoms were, the greater the AI exerted influence over somatosensory and motor regions (i.e., the posterior insula, right parietal operculum, and precentral gyrus), as well as over

brain areas involved in visuospatial processing (the paracingulate gyrus) and self-other processing (i.e., the anterior and posterior cingulate cortices, superior frontal gyrus and supramarginal gyrus). See **Figure 3**.

Table 2: Changes in the anterior insula effective connectivity between responder and nonresponder patients. Regions exhibiting a significant difference in *Granger causality analysis* maps between V1 and V7 according to treatment response. Coordinates are reported in MNI (Montreal Neurological Institute) space.

x	y	z	t	p	Label
-63	-45	36	-3.813837	0.000662	Left Supramarginal Gyrus. posterior division
-57	-30	39	-4.072859	0.000328	Left Supramarginal Gyrus. anterior division
-6	-39	45	-3.452251	0.001728	Cingulate Gyrus. posterior division
-3	30	27	-2.993126	0.005594	Cingulate Gyrus. anterior division
6	-72	42	3.098338	0.004296	Right Precuneus Cortex
21	-9	66	-3.458369	0.0017	Superior Frontal Gyrus
27	3	-12	-2.894758	0.007138	Right amygdala
45	0	9	-2.875736	0.007479	Right Central Opercular Cortex

INSERT FIGURE 2 AND FIGURE 3 ABOUT HERE

Intrinsic network spatial stability measure at V7

Finally, the assessment of the spatial stability of the DMN and CEN posttreatment revealed that the severity of "reexperiencing" symptoms was positively correlated with the DMN GoF scores (**r = 0.521, p = 0.003**) and negatively correlated with the CEN GoF scores (**r = -0.418 p = 0.021** - Cf. **Figure 3**).

DISCUSSION

The present fMRI study was designed to explore how an effective chemo-facilitated psychotherapy for intrusive symptoms in PTSD could modulate AI causal influences over the brain. Very limited fMRI studies measured pre/post treatment changes in PTSD (48) and to our knowledge, none of them included effective connectivity. We focused on the AI since this region is known to be: (i) a central integration hub serving sensory, emotional, motivational and cognitive functions, (ii) under B-noradrenergic regulation, and (iii) potentially involved in re-experiencing trauma. Using high temporal-resolution fMRI and comparing pre/post therapy GCA results in PTSD patients, we were able to provide evidence that treatment response was associated with a significant reduction in AI effective connectivity towards motor and socioaffective regions, a global decrease that follows symptom severity reduction.

The first set of regions modulated by AI corresponded to limbic areas for which dense reciprocal connections with the ventral AI were repeatedly described. A strong body of evidence supports AI mediation in fear and anxiety, which was regularly found to be coactivated with the amygdala in stressful contexts (9). By showing a reduced influence of AI on the amygdala in responders compared with nonresponders, we can assume that one of the first effects of treatment was to temper the emotional storm associated with reexperiencing and hyperarousal (18). This finding nicely complements the existing literature in which joint amygdalar and insular overactivation is described in the context of PTSD (20) and declines after successful psychotherapy (49). The ability to better modulate AI connectivity following therapy could be associated with better cross-talk between untargeted inner thoughts and the ability to focus attention on stimulus-dependent demands (50), a theory also supported by the association found between symptom severity and AI influence over visuospatial areas. Using GCA, we were able to attest that AI primarily drives this pathological interaction in PTSD.

The second set of brain areas modulated by AI are involved in self-other distinction and may support dissociative experiences frequently observed in PTSD. This is the case for the precuneus, frontal superior and supramarginal gyri, all regularly found to be involved in self-awareness and agency processing (e.g., (51)). These cognitive functions are more usually under the influence of the dorsal AI (52). Interestingly, localized AI lesions can induce dissociative experiences, such as the (rare) "pain asymbolia" syndrome, in which pain recognition appears disconnected from its appropriate emotional response (9). Within this functional network, the supramarginal gyrus, located at the temporo-parietal junction, has also been linked with experiences involving a sensorial component. Similar to the AI, the supramarginal gyrus receives heavy sensory inputs ranging from the auditory to the somatosensory modality. The crossmodal nature of this area makes it particularly well suited for linking sensory experiences with cognitive and/or affective information. Finally, the supramarginal gyrus is also involved in the phonological and articulatory processing of words (53), making it solicistable by talking therapy. Again, this is perfectly in line with the present findings showing that the AI influence on this network was correlated with the degree of intrusion and was significantly decreased in facilitated psychotherapy responders.

The third set of regions influenced by AI is engaged in sensorimotor control (54–56) and might be involved in the autonomic and behavioral responses to stress. Again, this interaction was found to correlate with symptom severity, even if only indirectly through the posterior insula and thalamic relays (57), which were found to be under AI control at baseline. The motor network under consideration includes the caudal anterior cingulate cortex (cACC), the supplementary motor area and the precentral gyrus. A decreased resting-state functional connectivity between the cACC and the precentral gyrus was previously evidenced in veterans with or without PTSD compared to healthy controls, suggesting that military training or deployment, including trauma exposure, may influence SN connectivity (58). In addition, precentral activity has been related to defensive behaviors in animals (59) and may subserve the increased "fight or flight" response regularly observed in PTSD when facing mental stress.

In addition to networks sustaining the rich phenomenology of PTSD symptoms, we also investigated how effective treatment may dynamically affect the interaction between intrinsic neural networks. We first demonstrated that the more the AI exerted a causal influence over core nodes of the DMN (such as the rostral ACC, the posterior cingulate and the precuneus), the more severe intrusive symptoms were, and that this interaction differentially changed at V7 according to the treatment response. This finding appears in line with previous studies conducted in schizophrenia patients (21), showing that increased control from the SN to the DMN initiates hallucinatory states. Interestingly, the DMN is also known to anti-correlate with task-related networks, such as the CEN (60,61), and this antagonistic activity was proposed to be tuned by the AI (22). Returning to our schizophrenia example, a CEN takeover was found to drive the extinction of hallucinations (21). Here, we found that reexperiencing the trauma positively correlated with DMN stability and presented a reversed pattern for the CEN. Altogether, these results support the idea that intrusive symptoms could correspond to self-referential mental activities driven by impaired AI control over the DMN/CEN balance, making salient memory fragments active enough (through bottom-up amplification) to aberrantly intrude into consciousness.

Despite these encouraging findings, some issues need to be further discussed. If the abovementioned theory is correct, we could expect to find the hippocampal complex among the regions influenced by the AI. The limited sample-size of the present trial may account for such a negative result (i.e., a power issue), and the exact relationship between the AI and this limbic structure will have to be clarified in future studies. In fact, several brain areas identified in this study have previously been shown to be involved in memory suppression beyond the medial temporal lobe. This is the case for the precuneus and the frontal cortex (62), which have tight connections with the hippocampus (63,64). The same is true for other limbic structures, such as the amygdala which have strong reciprocal connections with the hippocampus. We cannot exclude that intermediate small brain structures, such as the hippocampus, that are involved in a chain of causality could be more vulnerable and may not survive statistical thresholding. Based on that possibility, we

hypothesize a triple interaction [AI - amygdala - hippocampus] at the root of the memorization of trauma-related emotional valence, constituting an interesting complementary track for future research on PTSD.

A second potential issue resides in the fact that GCA indicates the dominant direction of influence, introducing ambiguity in the interpretation of pre/post treatment contrast maps, as they may potentially result from a decrease in the influence of AI-to-target-regions influence or from an increase in the influence of target-to-AI. This problem can, for instance, be illustrated by considering a recent study of effective connectivity in PTSD that reached seemingly opposite conclusions, suggesting that frontal regions exerted a reduced influence on AI (65). In the same vein, a decreased causal flow from the right amygdala to the right insula in PTSD patients relative to trauma-exposed controls has been suggested (23), which again appears in apparent contradiction with the present findings. Even if the samples and designs were not exactly comparable, methodological advances should help to reconcile these findings, but until then, this literature needs to be interpreted with caution and in reference to clinically and anatomo-functionally available knowledge at the time of publication.

A final point we would like to insist on is that we focused on symptom reduction, regardless of the initial group of randomisation in the *Pre-Reactivation Propranolol Therapy* trial. Of course, the full results of the RCT have been presented elsewhere (30) and are beyond the scope of the present paper. Note that the between-group differences were both explained by changes in the responder and nonresponder groups. This is compatible with previous studies showing that psychotherapy could induce functional changes, even in cases of no clinical response (48), that could be linked with repeated trauma exposure without extinction, as suggested in previous studies (58). Importantly, because half of the sample did not reach the threshold for a positive response to chemo-facilitated psychotherapy, we expect our findings to also be relevant for future neuromodulation trials for

severely impaired PTSD patients. In this vein, a recent study confirmed that such patients could be trained to downregulate amygdalar activity using real time fMRI-based neurofeedback (66).

Overall, we were able to provide experimental support for the causal role played by AI in reexperiencing trauma. Notably, we showed that effective facilitated psychotherapy was linked with plastic changes in AI directed influence over sensorimotor, cognitive and socioemotional networks. Dynamically, restoration of the DMN-to-CEN switch control was also observed, offering an attractive mechanism for intrusion. We hope that the present results will contribute to paving the way for new evidenced-based treatments of intrusive symptoms in PTSD, considering AI as a particularly interesting target for this purpose.

REFERENCES:

1. Horesh D, Brown AD (2020): Traumatic stress in the age of COVID-19: A call to close critical gaps and adapt to new realities. *Psychol Trauma Theory Res Pract Policy* 12: 331–335.
2. Lewis SJ, Arseneault L, Caspi A, Fisher HL, Matthews T, Moffitt TE, *et al.* (2019): The epidemiology of trauma and post-traumatic stress disorder in a representative cohort of young people in England and Wales. *Lancet Psychiatry* 6: 247–256.
3. American Psychiatric Association (2013): *Diagnostic and Statistical Manual of Mental Disorders,* Fifth Edition. American Psychiatric Association. https://doi.org/10.1176/appi.books.9780890425596
4. Brewin CR, Gregory JD, Lipton M, Burgess N (2010): Intrusive images in psychological disorders: characteristics, neural mechanisms, and treatment implications. *Psychol Rev* 117: 210–232.
5. Larøi F, Sommer IE, Blom JD, Fernyhough C, Ffytche DH, Hugdahl K, *et al.* (2012): The characteristic features of auditory verbal hallucinations in clinical and nonclinical groups: state-of-the-art overview and future directions. *Schizophr Bull* 38: 724–733.
6. Newman MG, Llera SJ, Erickson TM, Przeworski A, Castonguay LG (2013): Worry and generalized anxiety disorder: a review and theoretical synthesis of evidence on nature, etiology, mechanisms, and treatment. *Annu Rev Clin Psychol* 9: 275–297.
7. Watkins ER (2008): Constructive and unconstructive repetitive thought. *Psychol Bull* 134: 163–206.
8. van den Heuvel MP, Sporns O (2013): Network hubs in the human brain. *Trends Cogn Sci* 17: 683–696.
9. Gogolla N (2017): The insular cortex. *Curr Biol CB* 27: R580–R586.
10. Augustine JR (1996): Circuitry and functional aspects of the insular lobe in primates including humans. *Brain Res Rev* 22: 229–244.
11. Bamiou D-E, Musiek FE, Luxon LM (2003): The insula (Island of Reil) and its role in auditory processing: Literature review. *Brain Res Rev* 42: 143–154.
12. Butti C, Hof PR (2010): The insular cortex: a comparative perspective. *Brain Struct Funct* 214: 477–493.
13. Mesulam M-M, Mufson EJ (1982): Insula of the old world monkey. Architectonics in the insulo-orbito-temporal component of the paralimbic brain. *J Comp Neurol* 212: 1–22.
14. Nieuwenhuys R (2012): Chapter 7 - The insular cortex: A review. In: Hofman MA, Falk D, editors. *Progress in Brain Research*, vol. 195. Elsevier, pp 123–163.
15. Bushara, Grafman J, Hallett M (2001): Neural correlates of auditory-visual stimulus onset asynchrony detection. *J Neurosci Off J Soc Neurosci* 21: 300–304.
16. Bushara, Hanakawa T, Immisch I, Toma K, Kansaku K, Hallett M (2003): Neural correlates of cross-modal binding. *Nat Neurosci* 6: 190–195.
17. Menon, Uddin LQ (2010): Saliency, switching, attention and control: a network model of insula function. *Brain Struct Funct* 214: 655–667.
18. Yehuda R, Hoge CW, McFarlane AC, Vermetten E, Lanius RA, Nievergelt CM, *et al.* (2015): Post-traumatic stress disorder. *Nat Rev Dis Primer* 1: 15057.
19. Stevens JS, Reddy R, Kim YJ, van Rooij SJH, Ely TD, Hamann S, *et al.* (2018): Episodic memory after trauma exposure: Medial temporal lobe function is positively related to re-experiencing and inversely related to negative affect symptoms. *NeuroImage Clin* 17: 650–658.
20. Koch SBJ, van Zuiden M, Nawijn L, Frijling JL, Veltman DJ, Olff M (2016): Aberrant resting-state brain activity in posttraumatic stress disorder: a meta-analysis and systematic review. *Depress Anxiety* 33: 592–605.
21. Lefebvre S, Demeulemeester M, Leroy A, Delmaire C, Lopes R, Pins D, *et al.* (2016): Network dynamics during the different stages of hallucinations in schizophrenia. *Hum Brain Mapp* 37: 2571–2586.
22. Sridharan D, Levitin DJ, Menon V (2008): A critical role for the right fronto-insular cortex in switching between central-executive and default-mode networks. *Proc Natl Acad Sci U S A* 105: 12569–12574.
23. Weng Y, Qi R, Zhang L, Luo Y, Ke J, Xu Q, *et al.* (2019): Disturbed effective connectivity patterns in an intrinsic triple network model are associated with posttraumatic stress disorder. *Neurol Sci Off J Ital Neurol Soc Ital Soc Clin Neurophysiol* 40: 339–349.
24. Zerbi V, Floriou-Servou A, Markicevic M, Vermeiren Y, Sturman O, Privitera M, *et al.* (2019): Rapid Reconfiguration of the Functional Connectome after Chemogenetic Locus Coeruleus Activation. *Neuron* 103: 702-718.e5.
25. Onur OA, Walter H, Schlaepfer TE, Rehme AK, Schmidt C, Keysers C, *et al.* (2009): Noradrenergic enhancement of amygdala responses to fear. *Soc Cogn Affect Neurosci* 4: 119–126.
26. Cameron OG, Minoshima S (2002): Regional brain activation due to pharmacologically induced adrenergic interoceptive stimulation in humans. *Psychosom Med* 64: 851–861.

27. Hermans EJ, van Marle HJF, Ossewaarde L, Henckens MJAG, Qin S, van Kesteren MTR, *et al.* (2011): Stress-related noradrenergic activity prompts large-scale neural network reconfiguration. *Science* 334: 1151–1153.
28. Cousijn H, Rijpkema M, Qin S, van Marle HJF, Franke B, Hermans EJ, *et al.* (2010): Acute stress modulates genotype effects on amygdala processing in humans. *Proc Natl Acad Sci U S A* 107: 9867–9872.
29. Brunet A, Saumier D, Liu A, Streiner DL, Tremblay J, Pitman RK (2018): Reduction of PTSD Symptoms With Pre-Reactivation Propranolol Therapy: A Randomized Controlled Trial. *Am J Psychiatry* 175: 427–433.
30. Roullet P, Vaiva G, Véry E, Bourcier A, Yrondi A, Dupuch L, *et al.* (submitted): Traumatic memory reactivation with or without propranolol for PTSD and comorbid MD symptoms: A randomized clinical trial.
31. Ventureyra VAG, Yao S-N, Cottraux J, Note I, De Mey-Guillard C (2002): The validation of the Posttraumatic Stress Disorder Checklist Scale in posttraumatic stress disorder and nonclinical subjects. *Psychother Psychosom* 71: 47–53.
32. Brady F, Warnock-Parkes E, Barker C, Ehlers A (2015): Early in-session predictors of response to trauma-focused cognitive therapy for posttraumatic stress disorder. *Behav Res Ther* 75: 40–47.
33. Mushtaq D, Ali A, Margoob MA, Murtaza I, Andrade C (2012): Association between serotonin transporter gene promoter-region polymorphism and 4- and 12-week treatment response to sertraline in posttraumatic stress disorder. *J Affect Disord* 136: 955–962.
34. Liu G, Sobering G, Duyn J, Moonen CT (1993): A functional MRI technique combining principles of echo-shifting with a train of observations (PRESTO). *Magn Reson Med* 30: 764–768.
35. Neggers SFW, Hermans EJ, Ramsey NF (2008): Enhanced sensitivity with fast three-dimensional blood-oxygen-level-dependent functional MRI: comparison of SENSE-PRESTO and 2D-EPI at 3 T. *NMR Biomed* 21: 663–676.
36. van Gelderen P, Duyn JH, Ramsey NF, Liu G, Moonen CTW (2012): The PRESTO technique for fMRI. *NeuroImage* 62: 676–681.
37. Deshpande G, Hu X (2012): Investigating effective brain connectivity from fMRI data: past findings and current issues with reference to Granger causality analysis. *Brain Connect* 2: 235–245.
38. Esteban O, Markiewicz CJ, Blair RW, Moodie CA, Isik AI, Erramuzpe A, *et al.* (2019): fMRIPrep: a robust preprocessing pipeline for functional MRI. *Nat Methods* 16: 111–116.
39. Gorgolewski K, Burns CD, Madison C, Clark D, Halchenko YO, Waskom ML, Ghosh SS (2011): Nipype: a flexible, lightweight and extensible neuroimaging data processing framework in python. *Front Neuroinformatics* 5: 13.
40. Roebroeck A, Formisano E, Goebel R (2005): Mapping directed influence over the brain using Granger causality and fMRI. *NeuroImage* 25: 230–242.
41. Menon (2015): Salience Network. In: Toga AW, editor. *Brain Mapping*. Waltham: Academic Press, pp 597–611.
42. Laird AR, Fox PM, Eickhoff SB, Turner JA, Ray KL, McKay DR, *et al.* (2011): Behavioral interpretations of intrinsic connectivity networks. *J Cogn Neurosci* 23: 4022–4037.
43. Forman SD, Cohen JD, Fitzgerald M, Eddy WF, Mintun MA, Noll DC (1995): Improved assessment of significant activation in functional magnetic resonance imaging (fMRI): use of a cluster-size threshold. *Magn Reson Med* 33: 636–647.
44. Eklund A, Nichols TE, Knutsson H (2016): Cluster failure: Why fMRI inferences for spatial extent have inflated false-positive rates. *Proc Natl Acad Sci U S A* 113: 7900–7905.
45. Eickhoff SB, Stephan KE, Mohlberg H, Grefkes C, Fink GR, Amunts K, Zilles K (2005): A new SPM toolbox for combining probabilistic cytoarchitectonic maps and functional imaging data. *NeuroImage* 25: 1325–1335.
46. Greicius MD, Srivastava G, Reiss AL, Menon V (2004): Default-mode network activity distinguishes Alzheimer's disease from healthy aging: evidence from functional MRI. *Proc Natl Acad Sci U S A* 101: 4637–4642.
47. Beck AT, Steer RA, Carbin MG (1988): Psychometric properties of the Beck Depression Inventory: Twenty-five years of evaluation. *Clin Psychol Rev* 8: 77–100.
48. Simmons AN, Norman SB, Spadoni AD, Strigo IA (2013): Neurosubstrates of remission following prolonged exposure therapy in veterans with posttraumatic stress disorder. *Psychother Psychosom* 82: 382–389.
49. Malejko K, Abler B, Plener PL, Straub J (2017): Neural Correlates of Psychotherapeutic Treatment of Post-traumatic Stress Disorder: A Systematic Literature Review. *Front Psychiatry* 8: 85.
50. Szeszko PR, Yehuda R (2019): Magnetic resonance imaging predictors of psychotherapy treatment response in post-traumatic stress disorder: A role for the salience network. *Psychiatry Res* 277: 52–57.

51. Sperduti M, Delaveau P, Fossati P, Nadel J (2011): Different brain structures related to self- and external-agency attribution: a brief review and meta-analysis. *Brain Struct Funct* 216: 151–157.
52. Kurth F, Zilles K, Fox PT, Laird AR, Eickhoff SB (2010): A link between the systems: functional differentiation and integration within the human insula revealed by meta-analysis. *Brain Struct Funct* 214: 519–534.
53. Stoeckel C, Gough PM, Watkins KE, Devlin JT (2009): Supramarginal gyrus involvement in visual word recognition. *Cortex J Devoted Study Nerv Syst Behav* 45: 1091–1096.
54. Chouinard PA, Paus T (2006): The primary motor and premotor areas of the human cerebral cortex. *Neurosci Rev J Bringing Neurobiol Neurol Psychiatry* 12: 143–152.
55. Dum RP, Strick PL (1991): The origin of corticospinal projections from the premotor areas in the frontal lobe. *J Neurosci Off J Soc Neurosci* 11: 667–689.
56. Paus T (2001): Primate anterior cingulate cortex: where motor control, drive and cognition interface. *Nat Rev Neurosci* 2: 417–424.
57. Uddin LQ, Nomi JS, Hebert-Seropian B, Ghaziri J, Boucher O (2017): Structure and function of the human insula. *J Clin Neurophysiol Off Publ Am Electroencephalogr Soc* 34: 300.
58. Kennis M, Rademaker AR, van Rooij SJH, Kahn RS, Geuze E (2014): Resting state functional connectivity of the anterior cingulate cortex in veterans with and without post-traumatic stress disorder. *Hum Brain Mapp* 36: 99–109.
59. Graziano MSA, Cooke DF (2006): Parieto-frontal interactions, personal space, and defensive behavior. *Neuropsychologia* 44: 845–859.
60. Fox MD, Snyder AZ, Vincent JL, Corbetta M, Van Essen DC, Raichle ME (2005): The human brain is intrinsically organized into dynamic, anticorrelated functional networks. *Proc Natl Acad Sci U S A* 102: 9673–9678.
61. Greicius MD, Krasnow B, Reiss AL, Menon V (2003): Functional connectivity in the resting brain: a network analysis of the default mode hypothesis. *Proc Natl Acad Sci U S A* 100: 253–258.
62. Mary A, Dayan J, Leone G, Postel C, Fraisse F, Malle C, *et al.* (2020): Resilience after trauma: The role of memory suppression. *Science* 367. https://doi.org/10.1126/science.aay8477
63. Cunningham SI, Tomasi D, Volkow ND (2017): Structural and functional connectivity of the precuneus and thalamus to the default mode network. *Hum Brain Mapp* 38: 938–956.
64. Anderson MC, Bunce JG, Barbas H (2016): Prefrontal-hippocampal pathways underlying inhibitory control over memory. *Neurobiol Learn Mem* 134 Pt A: 145–161.
65. Rangaprakash D, Dretsch MN, Venkataraman A, Katz JS, Denney TS, Deshpande G (2018): Identifying disease foci from static and dynamic effective connectivity networks: Illustration in soldiers with trauma. *Hum Brain Mapp* 39: 264–287.
66. de Pierrefeu A, Fovet T, Hadj-Selem F, Löfstedt T, Ciuciu P, Lefebvre S, *et al.* (2018): Prediction of activation patterns preceding hallucinations in patients with schizophrenia using machine learning with structured sparsity. *Hum Brain Mapp* 39: 1777–1788.

FIGURES & TABLES

Figure 1. Study design and *Granger causality analysis* (GCA) seeded on the anterior insula in PTSD patients. (A) The bilateral anterior insula was chosen as the region of interest for GCA and is presented in red in a glass brain. **(B)** Flow chart of the study. We defined responders as patients with at least a 30% decrease in PCL-S scores at V7 compared with baseline (V1). **(C)** Whole-sample random-effects GCA map at V1. PCL-S: Posttraumatic Stress Disorder Checklist Scale; Thal: thalamus; Hipp: hippocampus; SMA: supplementary motor area; A: anterior; P: posterior; L/R: left/right sides of the brain.

Figure 2. Changes in *Granger causality* maps seeded on the anterior insula (AI) between responders and nonresponders to chemo-facilitated therapy in PTSD. We used a transparent right hemisphere to allow visualization of the deeper clusters. Brain areas less influenced by AI after effective treatment are depicted in dark blue. The precuneus (pink) was the only cluster found to be more influenced by AI posttreatment in responders than in nonresponders.

Figure 3. Brain correlates of intrusive symptom severity in PTSD. **(A)** Linear regression analysis showing the brain regions exhibiting a positive association between the severity of intrusive symptoms and thresholded *Granger causality analysis* maps at V7. **(B, C)** Correlation analyses between intrinsic network stability and the severity of intrusive symptoms at V7. A positive association was indicated by the default mode network stability (DMN GoF score), shown in **(B)**, whereas a negative association was indicated by the central executive network stability (CEN GoF score), shown in **(C)**.

Table 1: Population description.

Table 2: Changes in the anterior insula effective connectivity between responder and nonresponder patients. Regions exhibiting a significant difference in *Granger causality analysis* maps between V1 and V7 according to treatment response. Coordinates are reported in MNI (Montreal Neurological Institute) space.

SUPPLEMENTARY MATERIAL

Supplementary Figure 1. Changes in *Granger causality* maps seeded on the anterior insula (AI) in responders to chemo-facilitated therapy in PTSD (cortical clusters). Brain areas less influenced by AI after effective treatment are depicted in dark blue. Brain areas more influenced by AI after effective treatment are depicted in pink (i.e. dorsal anterior cingulate cortex, part of the salience network).

Supplementary Figure 2. Changes in *Granger Causality* maps seeded on the Anterior Insula (AI) in non-responders to chemo-facilitated therapy in PTSD (cortical clusters). Brain areas less influenced by AI after effective treatment are depicted in dark blue. Brain areas more influenced by AI after effective treatment are depicted in pink.

Supplementary table 1. Whole-sample *Granger causality analysis* seeded on the anterior insula at baseline. Coordinates are reported in MNI (Montreal Neurological Institute) space.

Supplementary table 2. Regions showing a significant (time-point x group) interaction for *Granger causality analysis* seeded on the anterior insula. Coordinates are reported in MNI (Montreal Neurological Institute) space.

Supplementary table 3. Regions influenced by the anterior insula showing a significant difference between V7 and V1 in responders. Coordinates are reported in the MNI (Montreal Neurological Institute) space.

Supplementary table 4. Regions influenced by the anterior insula showing a significant difference between V7 and V1 in nonresponders. Coordinates are reported in the MNI (Montreal Neurological Institute) space.

Supplementary table 5. Comparison of *Granger Causality* maps seeded the Anterior Insula at V7 between the propranolol facilitated therapy group and the placebo-controlled group. Coordinates are reported in the MNI (Montreal Neurological Institute) space.

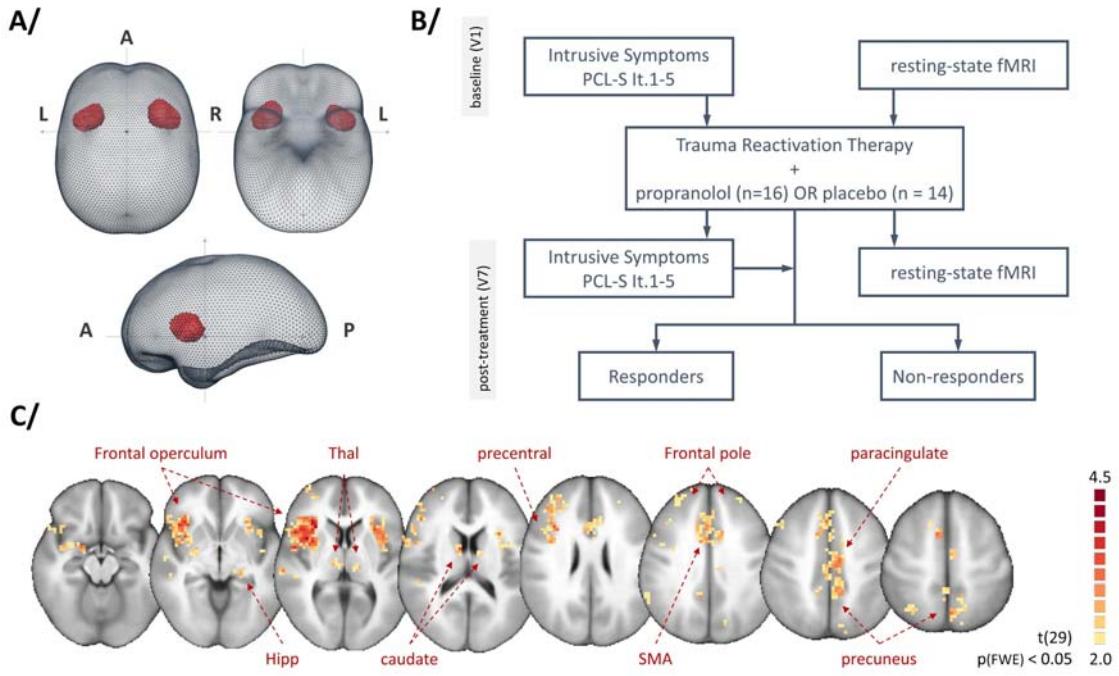

Figure 1. **Study design and *Granger causality analysis* (GCA) seeded on the anterior insula in PTSD patients.** **(A)** The bilateral anterior insula was chosen as the region of interest for GCA and is presented in red in a glass brain. **(B)** Flow chart of the study. We defined responders as patients with at least a 30% decrease in PCL-S scores at V7 compared with baseline (V1). **(C)** Whole-sample random-effects GCA map at V1. PCL-S: Posttraumatic Stress Disorder Checklist Scale; Thal: thalamus; Hipp: hippocampus; SMA: supplementary motor area; A: anterior; P: posterior; L/R: left/right sides of the brain.

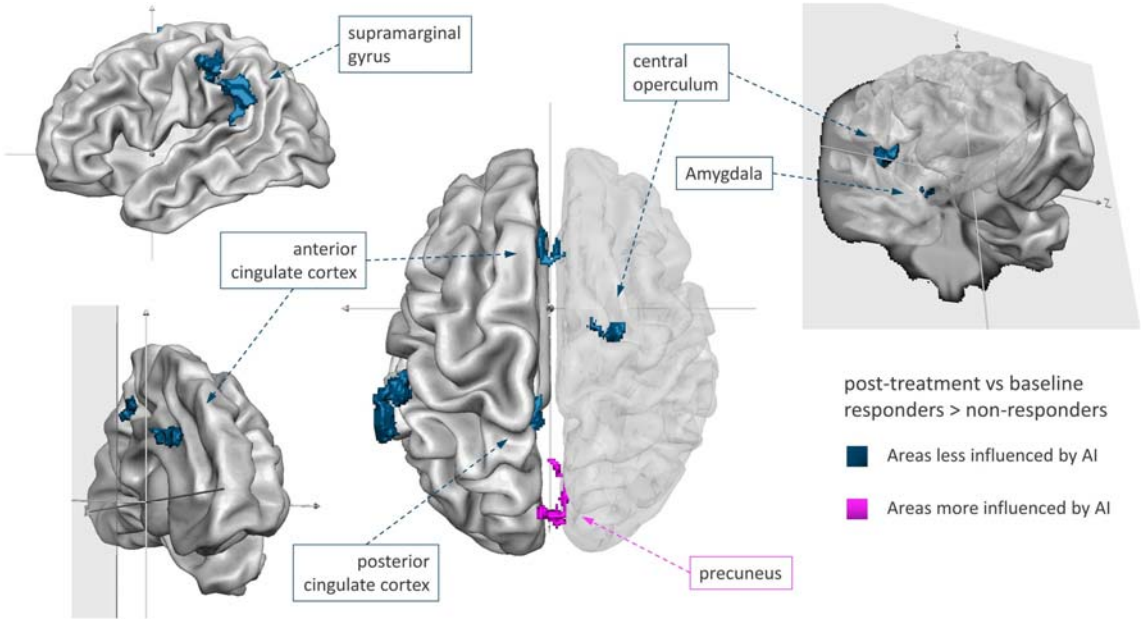

Figure 2. Changes in *Granger causality* maps seeded on the anterior insula (AI) between responders and nonresponders to chemo-facilitated therapy in PTSD. We used a transparent right hemisphere to allow visualization of the deeper clusters. Brain areas less influenced by AI after effective treatment are depicted in dark blue. The precuneus (pink) was the only cluster found to be more influenced by AI posttreatment in responders than in nonresponders.

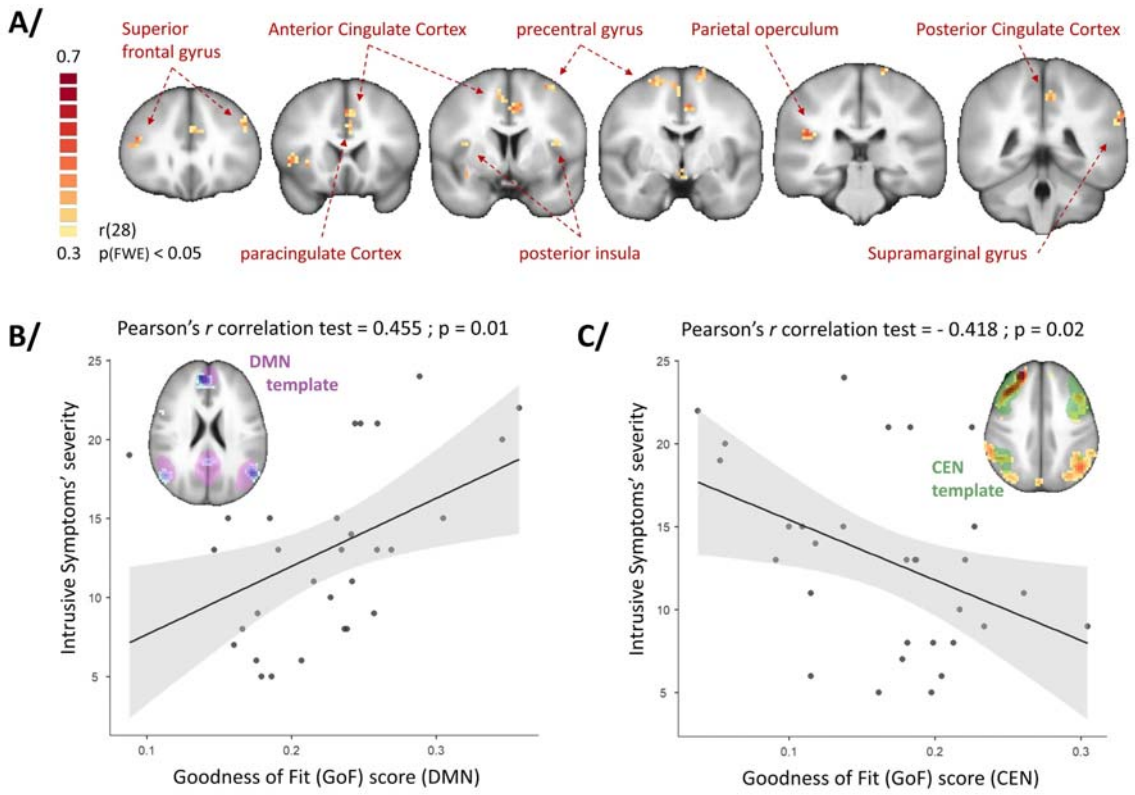

Figure 3. Brain correlates of intrusive symptom severity in PTSD. **(A)** Linear regression analysis showing the brain regions exhibiting a positive association between the severity of intrusive symptoms and thresholded *Granger causality analysis* maps at V7. **(B, C)** Correlation analyses between intrinsic network stability and the severity of intrusive symptoms at V7. A positive association was indicated by the default mode network stability (DMN GoF score), shown in **(B)**, whereas a negative association was indicated by the central executive network stability (CEN GoF score), shown in **(C)**.